Multiple stressors threaten the imperiled coastal foundation species eelgrass (*Zostera marina*) in Chesapeake Bay, USA

JONATHAN S. LEFCHECK[1] (iD), DAVID J. WILCOX[1], REBECCA R. MURPHY[2], SCOTT R. MARION[3] and ROBERT J. ORTH[1]

[1]*Virginia Institute of Marine Science, The College of William & Mary, Gloucester Point, VA 23062, USA,* [2]*University of Maryland Center for Environmental Science, Chesapeake Bay Program, Annapolis, MD 21403, USA,* [3]*Oregon Department of Fish & Wildlife, Marine Resources Program, Newport, OR 97365, USA*

Abstract

Interactions among global change stressors and their effects at large scales are often proposed, but seldom evaluated. This situation is primarily due to lack of comprehensive, sufficiently long-term, and spatially extensive datasets. Seagrasses, which provide nursery habitat, improve water quality, and constitute a globally important carbon sink, are among the most vulnerable habitats on the planet. Here, we unite 31 years of high-resolution aerial monitoring and water quality data to elucidate the patterns and drivers of eelgrass (*Zostera marina*) abundance in Chesapeake Bay, USA, one of the largest and most valuable estuaries in the world, with an unparalleled history of regulatory efforts. We show that eelgrass area has declined 29% in total since 1991, with wide-ranging and severe ecological and economic consequences. We go on to identify an interaction between decreasing water clarity and warming temperatures as the primary drivers of this trend. Declining clarity has gradually reduced eelgrass cover the past two decades, primarily in deeper beds where light is already limiting. In shallow beds, however, reduced visibility exacerbates the physiological stress of acute warming, leading to recent instances of decline approaching 80%. While degraded water quality has long been known to influence underwater grasses worldwide, we demonstrate a clear and rapidly emerging interaction with climate change. We highlight the urgent need to integrate a broader perspective into local water quality management, in the Chesapeake Bay and in the many other coastal systems facing similar stressors.

Keywords: climate change, eutrophication, global warming, nutrients, remote sensing, seagrass

Received 24 October 2016 and accepted 19 December 2016

Introduction

Identifying the drivers of environmental change and predicting their consequences is the preeminent scientific challenge of the Anthropocene (Halpern *et al.*, 2008). Marine systems in particular are experiencing rapid and often irreversible alterations as a consequence of human activities (Lotze *et al.*, 2006), and almost half of these changes can be attributed to multiple drivers (Lotze *et al.*, 2006; Halpern *et al.*, 2008). Despite the increasing recognition that global and local stressors often act jointly, rigorous empirical examples of this phenomenon are lacking at the large scales relevant to both the observed change and human well-being. This absence is particularly striking for temperate coastal ecosystems, which, ironically, support much of the world's human population. Instead, most of our understanding of coastal change comes from small-scale experiments and observations (Crain *et al.*, 2008, 2009),

or from tropical systems such as coral reefs (Gardner *et al.*, 2003; De'ath *et al.*, 2012). This knowledge gap vastly impedes our ability to predict and avert the impacts of global change on key population centers, particularly given the fact that stressors, and corresponding management actions, often occur at much larger scales.

Seagrasses in particular are extremely sensitive to global change, with losses exceeding 25% worldwide in just the last century (Orth *et al.*, 2006; Waycott *et al.*, 2009). Because of its global distribution close to major anthropogenic influences, and its habit of forming monospecific stands in shallow zones, eelgrass (*Zostera marina*) is acutely vulnerable to environmental stressors (Waycott *et al.*, 2009). Consequently, it has experienced declines in many locations, including in northern Europe (Giesen *et al.*, 1990; Frederiksen *et al.*, 2004), the northwestern Atlantic (Beem & Short, 2009; Costello & Kenworthy, 2011), and the western coast of the USA, particularly San Francisco Bay (Short & Wyllie-Echeverria, 1996). Nowhere, though, has eelgrass experienced more

Correspondence: Jonathan S. Lefcheck, tel. +1 804 684 7150, fax +1 804 684 7097, e-mail: jslefche@vims.edu

significant losses than in Chesapeake Bay, USA (Orth & Moore, 1983).

The Chesapeake Bay is one of the largest, most well-managed, and economically productive coastlines in the world, and is projected to support 20 million people by 2020 (Orth RJ, Dennison WC, Lefcheck JS, in review). Eelgrass has played a prominent role in both the ecology and economy of Chesapeake Bay, providing numerous functions and services, including nursery habitat for valuable fisheries species and shoreline stabilization (Table 1) (Orth RJ, Dennison WC, Lefcheck JS, in review). The abundance of eelgrass in Chesapeake Bay has fluctuated dramatically over the last century, with a pandemic wasting disease driving a well-documented decline in the 1930s, and recovery occurring through the 1960s (Cottam, 1934; Orth & Moore, 1984). It was during a single summer in 1972, however, that Tropical Storm Agnes – and the accompanying freshwater discharge – extirpated over 50% of the eelgrass population. This was a major disturbance from which Chesapeake Bay eelgrass populations have never truly recovered (Fig. 1) (Orth & Moore, 1983; Orth *et al.*, 2010).

Alongside increasing industrialization of the region in the 1960s, there emerged interest in the impact of human activities on eelgrass in Chesapeake Bay: specifically, nutrient runoff from agriculture, and the consequent eutrophication of nearshore waters (Orth & Moore, 1984; Kemp *et al.*, 2005). Several recent correlative analyses have proposed that declining water quality and subsequent changes in light availability may be the primary agent preventing recovery of eelgrass in Chesapeake Bay after Agnes (Orth *et al.*, 2010; Patrick & Weller, 2015). At the same time, parallel investigations conducted in only a single subestuary have uncovered a potential role for rising temperatures alongside reduced visibility in driving a recent decade-long decline of eelgrass (Moore & Jarvis, 2008; Moore *et al.*, 2014). Together, these studies suggest a role for multiple influences on the trajectory of Chesapeake Bay eelgrass, although their effects have yet to be generalized to the regional scale.
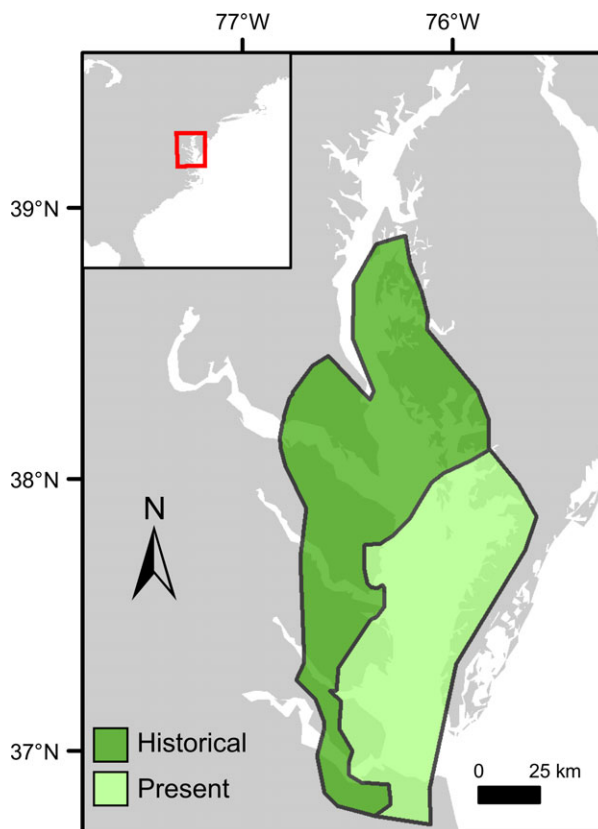
Fig. 1 Current (light green) and historical distribution (dark green) of eelgrass in Chesapeake Bay. Historical distribution is prior to 1971, immediately preceding Tropical Storm Agnes.

In this study, we use 31 years of high-resolution aerial imagery and water quality data to document the continued decline of eelgrass across the entirety of Chesapeake Bay, and directly link changes in its distribution to multiple anthropogenic stressors acting on the region. The scale, duration, comprehensiveness, and complementarity of these two datasets are unprecedented, and provide a unique opportunity to understand the specific drivers of habitat decline in a highly populated coastal system.

Table 1 Loss of ecosystem services concurrent with loss of eelgrass. Values are means $\pm$ 1 SD, estimated based on change in eelgrass cover from its peak in 1991 to present, and to the maximum observed loss in 2006.

Service	Response	Present loss (1991–2015)	Maximum loss (1991–2006)
Nutrient cycling	Carbon stock (kt C)	693 $\pm$ 150	1859 $\pm$ 401
	N_2 fixation (kt N)	2.53 $\pm$ 0.25	4.25 $\pm$ 0.16
Secondary production and export	Epifaunal biomass (Mt)	141.1 $\pm$ 75.2	236.6 $\pm$ 126.1
	Blue crab density (millions of juveniles)	523 $\pm$ 600	1403 $\pm$ 1609
	Silver perch biomass (kt)	47.8 $\pm$ 5.2	80.2 $\pm$ 8.8
Total economic loss	Integrated value ($2011 US)	$1.51 billion	$2.54 billion

Materials and methods

Eelgrass monitoring

Eelgrass bed area and density were derived from aerial imagery acquired on an annual basis from 1984 through 2015, except for 1988, from the Virginia Institute of Marine Science Submersed Aquatic Vegetation Monitoring Program (http://www.vims.edu/bio/sav). Panchromatic photography at a scale of 1 : 24 000; 60% flightline overlap and 20% sidelap was acquired with a standard mapping camera for 1984–2014. Multispectral imagery was acquired in 2014 and 2015 using a digital mapping camera with a ground sample distance of 24 cm. Acquisition conditions, including tidal stage, plant growth, sun angle, atmospheric transparency, water turbidity, and wind, were selected to optimize the visibility of eelgrass beds (Dobson et al., 1995).

Mapping of eelgrass beds was initially accomplished by manually tracing seagrass bed outlines onto translucent US Geological Survey 7.5-min quadrangle maps directly from the photographs, and then digitizing bed boundaries into a geographic information system (GIS) dataset for analysis. More recently, the aerial photography was scanned from negatives or produced digitally from the sensor and orthorectified using ERDAS LPS image-processing software (ERDAS, Atlanta, GA, USA). Eelgrass bed boundaries were then photo-interpreted directly on-screen while maintaining a fixed scale using ESRI ARCMAP GIS software (ESRI, Redlands, CA, USA). The spatial accuracy of the dataset varies from approximately ± 24 m for the earlier data to approximately ± 4 m for the recent data. Thematic accuracy has not been directly quantified, but has been improved through the use of extensive field observations.

A second species of seagrass, widgeongrass (Ruppia maritima), can co-occur with eelgrass in some locations of the lower Bay, or in monospecific stands (Orth & Moore, 1986). Any beds dominated by widgeongrass were excluded from the mapped area using expert knowledge, itself based on field surveys of the general distribution of the two species conducted since 1978. Thus, after the removal of these beds, we are confident that our analysis focuses specifically on eelgrass.

Water quality monitoring

Water quality data were obtained from the Chesapeake Bay Program's (CBP) Water Quality Database (http://www.chesapeakebay.net), which contains data collected in the tidal waters of Chesapeake Bay by agencies including Maryland Department of Nature Resources and Virginia Department of Environmental Quality. The program visits approximately 160 fixed monitoring stations every two weeks, 28 of which were used for our analysis (Fig. S1). At each station, a vertical hydrographic profile is collected using a multiparameter sonde with observations every 1–2 m of water temperature, specific conductivity (to calculate salinity), and dissolved oxygen. Secchi depth is observed in the field using a black-and-white Secchi disk attached to a measuring line. In addition, at each station, water samples are collected at several depths and processed at a laboratory to quantify concentrations of chlorophyll-a, total nitrogen, and total phosphorus. For this analysis, we used data only from the surface layer, the top 0.5 or 1 m observation, assuming these values best reflect conditions in the shallow water where eelgrass is present.

Methodological changes for chlorophyll-a, total nitrogen, and total phosphorus over the course of the survey necessitated the implementation of correction factors. Specifically, for nitrogen, the changes involved switching from a sum of nitrate, nitrite, and total Kjeldahl nitrogen to total dissolved nitrogen plus particulate nitrogen at Virginia mainstem stations in 1988, Maryland stations in 1998, and Virginia tributary stations in 1998. For phosphorus, the change involved switching from a sum of total dissolved phosphorus plus particulate phosphorus to a direct measurement in the same years as the total nitrogen changes. For chlorophyll-a, the possible changes occurred due to laboratories switches in the late 1990s, although it is likely this only impacted Virginia tributary stations. For these three variables, we regressed the response at each station against the identity of the processing laboratory and the method employed using simple linear regression. We then extracted the residuals from this relationship, and visual assessment of time series plots suggested that they adequately accounted for the a priori influence of laboratory and method. The residuals for these three variables were carried through all subsequent analyses.

While these stations are largely in deep water, many prior studies have shown that they can be adequately extrapolated to predict underwater vegetation in shallow areas (Li et al., 2007; Rybicki & Landwehr, 2007; Ruhl & Rybicki, 2010; Gurbisz & Kemp, 2014; Patrick et al., 2014, 2016). Even if the stations under- or over-represent conditions at shallow depths, the relative differences among stations and years are preserved, such that any inferences about the directionality and relative impact of the environmental variables should be unaffected.

Statistical analysis

A cell-based model with a cell size of 30 m was used to facilitate the analysis of eelgrass. Within the study area, ESRI ARCGIS software was used to code each 30 m cell in one of the following categories on the Braun-Blanquet cover scale: none (0% cover), very sparse (<10% cover), sparse (11–40% cover), moderate (41–70%), or dense (71–100%) (Paine, 1981). Additionally, we quantified the depth of the cell extracted from the Chesapeake Bay, VA/MD (M130) Bathymetric Digital Elevation Model (NOAA, http://estuarinebathymetry.noaa.gov/). For each grid cell, we then calculated the overwater distance to the nearest CBP monitoring station, and grouped all cells based on their nearest station, which we refer to as 'subregions' (Fig. S1). For each station, we calculated the total density-weighted eelgrass cover as the sum of the bottom area of the nearest grid cells, weighted by the Braun-Blanquet density, and merged these with the environmental data. This procedure yielded $n = 684$ observations for use in our modeling exercise.

We used the following generalized additive mixed model to identify the significant predictors of eelgrass cover:

$$y_{ij} = X_{ij} * \alpha + \sum_{k=1}^{p} f_k(x_{ij}) + Z_{ij}b_{ij} + Z_{i,j}b_i + \epsilon_{ij}$$

$$b_i = N(\mathbf{0}, \mathbf{\Psi}_1)$$

$$b_{ij} = N(0, \sigma_2^2)$$

$$\epsilon_{ij} = N(0, \sigma^2 I)$$

where the response y_{ij} is the $\log_{10}$-transformed density-weighted total cover of eelgrass in subregion i in year j, X_{ij} is the design matrix of parametric components and α is the vector of fixed effects parameters, $f_k(\cdot)$ are the nonparametric smoothed functions of covariates x_{ij}, Z_{ij} is the design matrix of the random effect of region i in year j and b_{ij} is the corresponding vector of random effects (for region designations, see Fig. S1), $Z_{i,j}$ is the design matrix of the random effect of year j on the measurements for region i in year j and b_i is the corresponding vector of random effects, and ε_{ij} is the within-region and within-year error independent of the random effects. All random effects and residual error are assumed to be normally distributed with a mean of 0, and positive definite variance–covariance matrices $\mathbf{\Psi}_1$, σ_2^2, and $\sigma^2 I$.

For the nonparametric component:

$$\sum_{k=1}^{p} f_k(x_{ij}) = f_1(\text{Long}, \text{Lat}) + f_2(\text{Cover}_{i(j-1)}) + f_3(\text{Habitat}_i)$$

$$+ f_4(\text{Chl}a_{ij}) + f_5(\text{Salinity}_{ij}) + f_6(\text{Secchi}_{ij}) + f_7(\text{TN}_{ij})$$

$$+ f_8(\text{TP}_{ij}) + f_9(\text{Temp}_{i(j-1)}) + f_{10}(\text{MaxTemp}_{i(j-1)})$$

$$+ f_{11}(\text{Secchi}_{ij}, \text{Temp}_{i(j-1)})$$

where all predictors are modeled as smoothing functions using the default thin-plate regression spline in the MGCV package in R (Wood, 2011). $f_1(\text{Long}, \text{Lat})$ is a smoothed combination of spatial coordinates using the UTM projection and is meant to address any potential spatial autocorrelation among the subregions. $f_2(\text{Cover}_{i(j-1)})$ represents eelgrass cover in subregion i in the previous year $j-1$, to account for the dependency of eelgrass cover from one year to the next. We fit this predictor as a smoothed covariate in lieu of a fixed autoregressive structure, having tested various combinations using model comparisons and visual examination of (partial) residual autocorrelation functions, and finding them to be less supported than simply modeling the previous year's eelgrass cover. $f_3(\text{Habitat}_{ij})$ represents the total available bottom for eelgrass with subregion i extending to 1 m Mean Low Water.

The remaining predictors are environmental variables summarized from the CBP Monitoring Program. Chlorophyll-*a*, salinity, Secchi depth, total nitrogen (TN), and total phosphorus (TP) were calculated as means for February to June in subregion i of year j, as we expected eelgrass to respond most strongly to these parameters during the growing season. The two predictors pertaining to temperature, $f_9(\text{Temp}_{i(j-1)}) + f_{10}(\text{MaxTemp}_{i(j-1)})$, were calculated as the mean and maximum values, respectively, from July to

September of the previous year $j-1$, as this is the time during which eelgrass undergoes natural temperature-driven senescence in this region (Moore & Jarvis, 2008). The final term is a combination of mean temperature and Secchi depth, estimating their interactive influence on cover independent of their main effects using a tensor product moment interaction smoother.

The model was constructed in R version 3.3.1 (R Development Core Team, 2016) using the MGCV package (Wood, 2011). The model was fit using restricted maximum likelihood (REML) to avoid overfitting and yield less biased estimates of the fixed effects, given the complexity of the model and the size of the dataset. Model assumptions of normality of errors and constant variance were assessed visually. Model predictions and 95% confidence intervals were obtained using the custom function *EvaluateSmooths* modified from StackOverflow (https://stackoverflow.com/questions/19735149/is-it-possible-to-plot-the-smooth-components-of-a-gam-fit-with-ggplot2), and from a modified version of the function PVISGAM in the ITSADUG package (van Rij *et al.*, 2016). We held a Type I error threshold of $\alpha = 1.05$. All data and scripts necessary to reproduce the analyses and generate all graphics are provided as Appendices S1–S3.

Ecosystem services and valuation

To estimate the potential ecological and economic losses associated with the decline of eelgrass, we collated *in situ* measurements of functioning from Chesapeake Bay eelgrass beds of the last decade (Table 1).

Data for estimation of total carbon loss were derived from *in situ* measurements of carbon stock as part of the Zostera Experimental Network (http://zenscience.org). Sediment core tubes (length: 50 cm, diameter: 50 mm) were forced to a depth of 30–40 cm into the sediment at a minimum distance of 15 m from each other at Goodwin Island, York River, extracted, and returned to the laboratory on ice. The samples were then dried and shipped to University of Southern Denmark, where samples were analyzed for sediment δ^{13} C, δ^{15} N, PON, and POC using a mass spectrometer (Thermo Scientific, delta V advantage, isotope ratio mass spectrometer). The measured isotope ratios were represented using the δ-notation with Vienna Peedee belemnite as reference material. Values of POC obtained by depth integration of the carbon density (mg C cm^{-3}) of 0–25 cm sediment layers were converted to carbon stock per unit sediment (mg C cm^{-2}), and averaged across $n = 3$ samples. We then averaged across all samples to yield a mean and standard deviation.

Estimates of N$_2$ fixation were obtained from Cole (2011), which reports estimates of whole system nitrogen flux, including the plant itself, epiphytes, and the sediment. In the publication, the author reports N$_2$ fixation rates as 3.9–5.8 g N m^{-2} yr^{-1}. From this range, we obtained an average by taking the difference and dividing it by two, and adding it to the lesser value, yielding 4.85 g N m^{-2} yr^{-1}.

Estimates of epifaunal invertebrate biomass per unit area were obtained from a long-running field survey at Goodwin Island, York River, Chesapeake Bay, from 2004 to 2012

(Douglass *et al.*, 2010). Ten grab samples per month collected epifauna over an area equivalent to 400 cm^2 of bottom. Animals in each sample were size fractionated, and biomass was estimated in mg ash-free dry mass using linear equations in (Edgar, 1990). These values were then averaged across all months and years to produce a mean and standard errors.

Juvenile blue crab abundance per unit area was obtained from (Ralph *et al.*, 2013). Values were averaged across all sampling locations to yield approximately 24 individuals m^{-2}, and standard deviations derived from standard error of the mean multiplied by the square root of the total sample size. To estimate economic losses associated with changes in blue crab abundance, a market price of \$US 3418 per metric ton was obtained from NOAA Office of Science and Technology Annual Commercial Landing Statistics (NOAA Office of Science and Technology, 2014) for the most recent available year (2014), including both hard- and soft-shelled individuals. We assumed an average adult mass of 150 g, and a conservative 10% catchability arising from a combination of postjuvenile mortality and fishing effort.

Estimates of silver perch production were obtained from (Sobocinski & Latour, 2015). We used a mean value of 91.5 g m^{-2} yr^{-1}, and obtained standard errors from the range 77.8–117.8 g m^{-2} yr^{-1} using the range rule, as above. Information on the fishery harvest of approximately 5900 mt yr^{-1} from the period of 2004–2014 also came from Sobocinski & Latour (2015).

Finally, estimates of total economic loss were obtained from Costanza *et al.* (2014), and as with all of the above estimates, assumes a 'basic benefit transfer' implying that the value of the service remains consistent per unit area. These values integrate across a range of potentially economically valuable services including provisioning of food and materials, bioprospecting, regulation of air, water, and climate, nursery services, and cultural, recreational and spiritual benefits (de Groot *et al.*, 2012). We used the 2011 valuation of \$28916 ha^{-1} yr^{-1} for combined seagrass/algal beds, noting that eelgrass beds can accumulate vast quantities of macroalgae.

For all values, we extrapolated to the total area lost multiplied by the period of time considered (30 years, if to present, or 22, if to the greatest observed loss). For nitrogen fixation and silver perch production, standard deviations were approximated by taking the difference of the range and dividing by 4, or the 'range rule'.

Results

From a peak in 1991, representing the maximum recovery post-Agnes, total eelgrass cover has declined by 29% to date (Fig. 2a). Moreover, the mean depth of eelgrass beds has declined by 0.12 m, or 26%, with most change occurring abruptly in 1997 (Fig. 2b). This change represents a greater loss of deep beds, which were reduced by 50%, vs. shallow beds, which actually increased in cover by 35% (Fig. 2c). Eelgrass beds have therefore shifted 165 m closer to shore since 1984 (Fig. 2d). Together, these results depict classic 'habitat squeeze', with eelgrass retreating into shallow water refugia where conditions are still favorable for growth, and all but eliminated in many areas >0.5 m depth where it was once abundant.

The widespread decline in eelgrass cover after 1991 appears to have been gradual until the early 2000s, after which point several acute diebacks occurred (Fig. 2a). The most extreme loss occurred in 2006, with a catastrophic 58% decline in total cover from the previous year, and a 78% decline from peak cover. Interestingly, eelgrass appeared to recover rapidly after these declines. Following the 2006 dieback, eelgrass cover increased by 55% over the previous year, and by 2009, had reached total cover exceeding that observed immediately prior to the dieback. A similar scenario occurred in 2011, where a less severe but still substantial decline of 41% reached pre-dieback area in less than two years. Our observations suggest eelgrass is responding to multiple drivers, one halting its recovery in the early 1990s and impacting eelgrass over the longer term, and another, more episodic driver beginning in the mid-2000s that relaxes enough to permit rapid recovery.

To clarify the correlates of changes in eelgrass abundance, we constructed a generalized additive mixed model (GAMM) incorporating 10 spatial, temporal, and environmental variables that together explained 84.6% of the variance in eelgrass cover. Beyond the expected influence of space and time, Secchi depth (an indicator of water clarity), mean water temperature of the preceding summer, and their interaction were the only other significant predictors of eelgrass cover ($P = 0.006$, $P < 0.001$, and $P = 0.029$; Fig. 3).

Decreasing Secchi depth (i.e., low visibility) is predicted to reduce eelgrass cover (Fig. 3a), and has declined by 30 cm since the beginning of the survey (Fig. 3b). Light is the principal factor governing eelgrass growth (Dennison, 1987), and our analysis confirms the long-running hypothesis that reduced water clarity is driving the long-term decline of eelgrass in Chesapeake Bay (Kemp *et al.*, 2004; Orth *et al.*, 2010), and in many other locations (Giesen *et al.*, 1990; Short & Wyllie-Echeverria, 1996). Average Secchi depth dropped below 1.5 m in 1997 (dashed line, Fig. 3b), exactly when the most abrupt change in eelgrass depth distribution occurred (Fig. 2b). This value constitutes the minimum depth limit recommended for this species in Chesapeake Bay, based on their known light requirements (Dennison *et al.* 1993). It therefore explains why deep beds have exhibited the strongest decline (Fig. 2c), as light penetration decreases exponentially with depth (Dennison, 1987). To confirm this hypothesis, we refit GAMMs for each depth strata to show that Secchi depth is the only significant predictor of eelgrass cover at depths >0.5 m MLW ($P = 0.020$; Fig. S2).
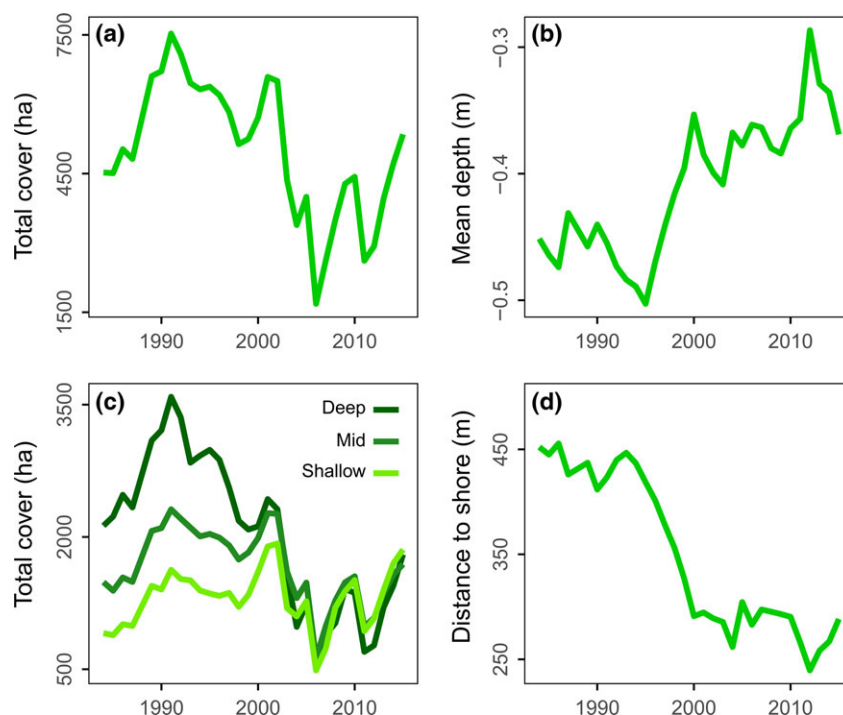
Fig. 2 Thirty-year trends in eelgrass cover and distribution. (a) Total cover (hectares) has been decreasing since 1991. (b) Mean depth of eelgrass beds has been decreasing since 1996. (c) The greatest loss has occurred in the deepest beds (deep = >0.5 m, mid = 0–0.5 m, shallow = 0 m). (d) Eelgrass has shifted 165 m closer to shore since 1984.

Increasing mean summer temperatures also reduced eelgrass cover, but only when exceeding 25 °C (Fig. 3c), a well-described threshold for mortality in this species (Zimmerman *et al.*, 1989; Reusch *et al.*, 2005; Moore *et al.*, 2014). Not only has the average summertime temperature increased from 24.9 to 26.4 °C since 1984, but the frequency of extreme mean temperatures (>28 °C) has also doubled in the last decade (dashed line, Fig. 3d), generalizing recent conclusions about the role of episodic heat events in driving localized diebacks (Moore & Jarvis, 2008). Thus, warming is the most likely driver behind more recent declines (Fig. 2a), particularly in shallow waters where light is not limiting (Fig. 2c). Indeed, GAMMs fit to individual depth strata show a significant effect of temperature only at intermediate and shallow depths (0–5 m, $P = 0.008$ and $P = 0.043$; Fig. S2).

Most importantly, we show that temperature and clarity interactively reduce eelgrass cover beyond what is expected from either alone (Fig. 4). A 2 °C increase in temperature, which is the low end of expectations for the Chesapeake Bay in the next 30 years (Najjar *et al.*, 2010), would result in a further decline in total eelgrass cover of 38%, holding all else constant. Similarly, if Secchi depth continues its trajectory and is reduced by another 40% over the next 30 years, it would result in a further decline of 84%. However, combined changes in temperature and Secchi depth would result in an expected loss of 95%, or the near total eradication of eelgrass in the Chesapeake Bay. While these values are based only on our model, and do not integrate any biology or account for continued management actions to reduce inputs into the Bay, it demonstrates potential for catastrophic losses as a result of the joint influence of these two stressors.

Finally, from independent *in situ* measurements in Chesapeake Bay eelgrass beds, we show loss of eelgrass has had severe consequences for ecosystem functioning and the provision of services relevant to human well-being (Table 1). For example, the total loss of carbon in sediments is estimated at 693–1859 kt C. Given the current social cost of carbon (Domestic Policy Council, 2013), this equates to an expected economic loss of \$US 96.5–259 million. Similarly, loss of eelgrass is expected to lead to a reduction of 523–1403 million juvenile blue crabs. Assuming a conservative 10% harvestable yield and the 2014 market price (NOAA Office of Science and Technology, 2014), this equates to a total potential economic loss of \$US 28.6–76.7 million. This value represents 1–2 years of the fishery, and even then does not account for consequent losses in recruitment in subsequent years. Similarly, the expected loss of silver perch equates to 10–20 years of the fishery (Sobocinski & Latour, 2015).
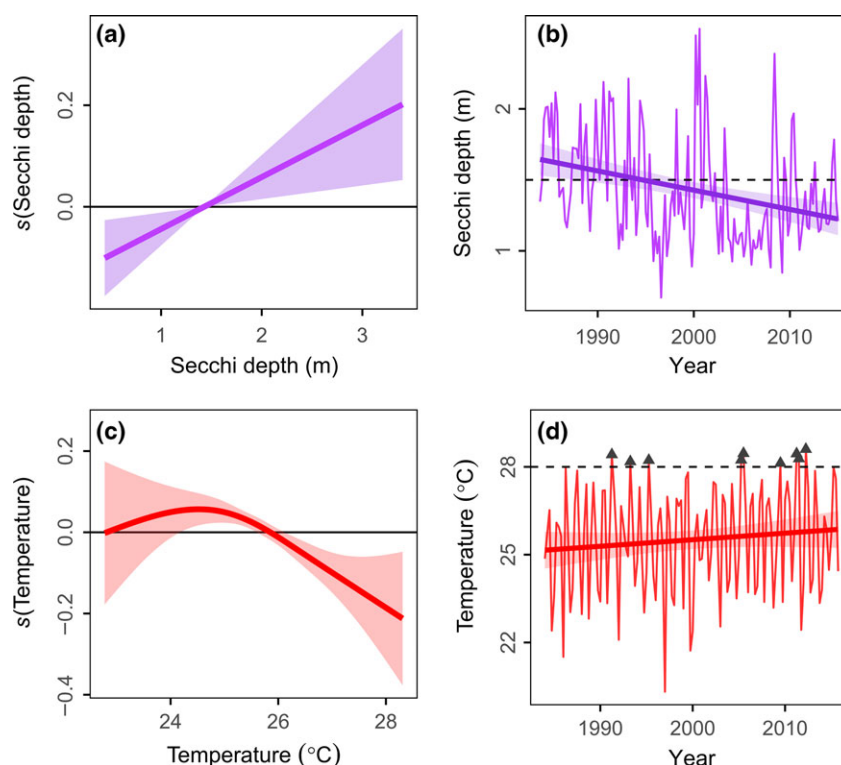
Fig. 3 Significant predictors of total eelgrass area based on a generalized additive mixed model. (a) Predicted cover increases with increasing Secchi depth, a measure of water clarity. Values on the *y*-axis represent the partial smoothed residuals accounting for the influence of the other predictors in the model. Shaded areas indicate 95% confidence intervals. (b) Water clarity has decreased by about 0.4 m over the past 30 years. Solid line denotes the predicted fit ± 95% CIs from simple linear regression. (c) Predicted cover decreases with increasing summer temperature. (d) Mean summertime temperature (July–September) has increased over the past 30 years, with a more recent rise in extreme temperature events (>28 °C, triangles).

In all, an independent and integrated measure of economic valuation (Costanza *et al.*, 2014) places the total potential economic loss due to the decline of eelgrass in Chesapeake Bay at $US 1.51–2.54 billion. Although these values are estimates extrapolated from small-scale data uninformed by the well-described variation in these services through time and space (Ralph *et al.*, 2013; Duffy *et al.*, 2015), and therefore must be interpreted with caution, they represent the best available data for assessing the outcome of eelgrass decline for the ecological and economic well-being of the Chesapeake Bay.

Discussion

Since the early 1990s, we show that eelgrass abundance in Chesapeake Bay has undergone a steady deterioration, punctuated by periods of intense decline (Fig. 2a). We propose that the long-term gradual declines are a consequence of declining water clarity, which has all but eliminated eelgrass beds deeper than 1 m where light is already limiting (Fig. 2c; Fig. S2). As the influence of clarity was independent of nutrients or

chlorophyll-*a* in our model, we propose that its effect stems from increased sediment loading, resuspension, and dissolution of organic matter due to greater watershed development and urbanization (Gallegos, 2001; Kemp *et al.*, 2004; Orth RJ, Dennison WC, Lefcheck JS, in review). At the same, we demonstrate that increasing summertime temperatures are behind episodic declines in 2005 and 2010, but are sufficiently infrequent, at this time, as to allow recovery (Fig. 2a). Critically, high temperatures appear to impact shallow beds more than deep ones (Fig. S2), suggesting that warming, and its interaction with clarity, is the most prominent threat for remaining eelgrass in Chesapeake Bay.

Warming has two implications for the persistence of eelgrass in Chesapeake Bay. First, it has been shown that rising temperatures elevates respiratory load, increasing light requirements for photosynthesis to balance metabolic demand, and exacerbating the negative effects associated with decreasing clarity (Zimmerman *et al.*, 1989; Zimmerman, 2006). Seagrasses, in general, have among the highest light requirements of any extant plants, primarily because of the need to support the large biomass of roots and rhizomes in a
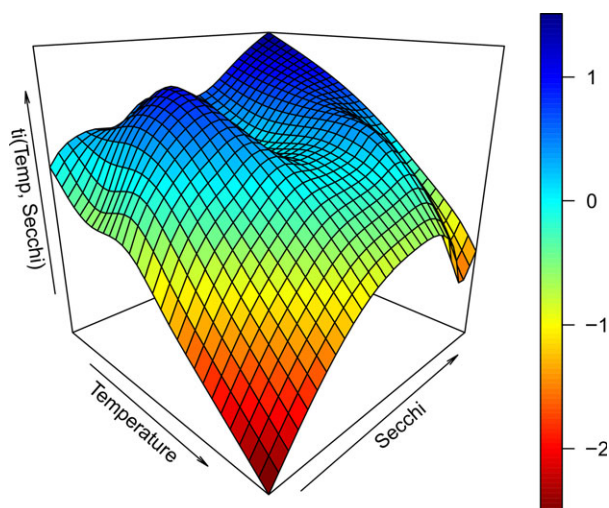
Fig. 4 Interaction surface between temperature and Secchi depth from a generalized additive mixed model. Eelgrass cover is predicted to decline when temperature is high and Secchi depth is low (bottom center). Values on the *y*-axis represent the partial residuals of the tensor product (ti) smoother accounting for the influence of the other predictors in the model.

sedimentary environment of low to no oxygen (Dennison *et al.*, 1993). Thus, the relationship between maximum depth distribution and Secchi depth has been well-documented, particularly in Chesapeake Bay (Dennison *et al.*, 1993). Consistent with this hypothesis, we show a highly significant interaction between the two such that the strongest declines in eelgrass are expected when temperature is maximal and Secchi depth is at its minimum (Fig. 4).

Second, eelgrass propagates both sexually, via seeds, and asexually, via clonal growth. When local populations dieback as a consequence of heat stress, the seedbank from the previous year permits rapid recolonization. However, diebacks in two consecutive years would fail to replenish the seedbank, as eelgrass seedlings in Chesapeake Bay flower in the second year of growth and seeds do not remain viable for more than a year, excluding any possibility of recovery (Jarvis & Moore, 2010). This scenario is not accounted for in our model and may result in the rapid and unpredictable eradication of eelgrass far more quickly than our analytical scenarios would otherwise suggest.

While eelgrass has stalled on its track of recovery since 1991, over the short term it has actually increased in abundance (Fig. 2a). We note, however, that cover observed at any point during this survey is only a fraction of what it was prior to the 1970s (Fig. 1), and more critically, is now restricted to only the most nearshore areas (Fig. 2c). Losses prior to this survey are also known to have come from pulse events, namely storms and disease, and have generally recovered within a

decade or two (Orth & Moore, 1983; Orth *et al.*, 2010). In contrast, we demonstrate a strong anthropogenic component in driving the continued and contemporary decline of eelgrass through degradations in water quality, warming, and their interaction. Therefore, we temper optimism of this recent upswing, and caution that without continued intervention to mitigate human impacts, principally those that affect light availability, eelgrass is unlikely to even reach coverage observed in the early 1990s, let alone historical maximums (Fig. 1). This point is critical considering those maximums have been used to set management targets for cover of underwater grasses in the polyhaline region of the Bay (Orth *et al.*, 2010, Orth RJ, Dennison WC, Lefcheck JS, in review).

Our study contributes to a general pattern of fragility among coastal ecosystems for which long-term regional records exist, including the Great Barrier and Caribbean coral reefs (Gardner *et al.*, 2003; De'ath *et al.*, 2012), kelp forests (Wernberg *et al.*, 2016), salt marshes (Jefferies *et al.*, 2006), and mangroves (Fromard *et al.*, 2004; Cavanaugh *et al.*, 2014). It also provides the most spatially and temporally comprehensive assessment of the patterns and drivers of decline in any seagrass species (Waycott *et al.*, 2009), and for one the largest, most productive, and valuable estuaries in the world (Orth *et al.*, 2017; Orth RJ, Dennison WC, Lefcheck JS, in review). Most importantly, we generalize mechanisms of seagrass decline derived from small-scale experiments and local observations to the scale of the entire Chesapeake Bay, principally sensitivity to declining water clarity and physiological intolerance to warming temperatures. This finding suggests that these mechanisms may be scale invariant and that experiments conducted in other systems could be reasonably extrapolated to predict regional abundance of eelgrass elsewhere, at least where physiological intolerances are similar to those exhibited in Chesapeake Bay.

Instead of facilitating decline, as we demonstrate here, climate change has been shown to mediate turnover in foundational species in many other examples, such as the ongoing replacement of marshes by mangroves in the southeastern USA (Cavanaugh *et al.*, 2014). In contrast with our study, there is no obvious candidate to supplant eelgrass in the Chesapeake Bay. Only one underwater grass coexists with eelgrass in the region, widgeongrass (*Ruppia maritima*), but it is generally restricted to shallow waters and so far has failed to establish in any abundance in areas vacated by eelgrass (Orth *et al.*, 2010). Rather, lost beds have by and large reverted to bare sediment, the least productive marine habitat (Duarte & Cebrián, 1996). Thus, the current crisis for eelgrass in Chesapeake Bay represents an almost total loss of functionality, echoing recent findings from systems such as coral reefs, where the transition to an

algal-dominated state has reduced or eliminated many of the same habitat and provisioning services (Graham & Nash, 2013).

Managers have long recognized that local-scale degradation of water clarity negatively affects many species of underwater grasses, not just eelgrass, from the Chesapeake Bay to the Gulf of Mexico, San Francisco Bay, and Australia (Giesen *et al.*, 1990; Short & Wyllie-Echeverria, 1996; Orth *et al.*, 2006; Waycott *et al.*, 2009). However, few if any implement strategies that account for rising temperatures in attempting to avert losses due to reduced water quality, despite mounting evidence of temperature-induced diebacks (Waycott *et al.*, 2009), even in places as far north as the Baltic Sea (Reusch *et al.*, 2005). This failure may explain the accelerating decline of seagrass species over the last century despite increasing awareness and intervention (Waycott *et al.*, 2009). Since climate change is a global phenomenon, we propose that managers must increase their water quality targets at the local and regional levels to offset losses caused by global factors outside their immediate control. Indeed, our model predictions show that given sufficient water clarity, eelgrass could still persist in the face of moderate increases in temperature. Only by adopting such an integrative perspective can we protect and restore eelgrass in the Chesapeake Bay, and elsewhere.

Acknowledgements

References

Beem NT, Short FT (2009) Subtidal eelgrass declines in the Great Bay Estuary, New Hampshire and Maine, USA. *Estuaries and Coasts*, **32**, 202–205.

Cavanaugh KC, Kellner JR, Forde AJ, Gruner DS, Parker JD, Rodriguez W, Feller IC (2014) Poleward expansion of mangroves is a threshold response to decreased frequency of extreme cold events. *PNAS*, **111**, 723–727.

Cole LW (2011) *Inputs and fluxes of nitrogen in the Virginia coastal bays: Effects of newly-restored seagrasses on the nitrogen cycle.* University of Virginia, 1–129 pp.

Costanza R, de Groot R, Sutton P *et al.* (2014) Changes in the global value of ecosystem services. *Global Environmental Change*, **26**, 152–158.

Costello CT, Kenworthy WJ (2011) Twelve-year mapping and change analysis of eelgrass (*Zostera marina*) areal abundance in Massachusetts (USA) identifies statewide declines. *Estuaries and Coasts*, **34**, 232–242.

Cottam C (1934) Past periods of eelgrass scarcity. *Rhodora*, **36**, 261–264.

Crain CM, Kroeker K, Halpern BS (2008) Interactive and cumulative effects of multiple human stressors in marine systems. *Ecology Letters*, **11**, 1304–1315.

Crain CM, Halpern BS, Beck MW, Kappel CV (2009) Understanding and managing human threats to the coastal marine environment. *Annals of the New York Academy of Sciences*, **1162**, 39–62.

De'ath G, Fabricius KE, Sweatman H, Puotinen M (2012) The 27-year decline of coral cover on the Great Barrier Reef and its causes. *PNAS*, **109**, 17995–17999.

Dennison WC (1987) Effects of light on seagrass photosynthesis, growth and depth distribution. *Aquatic Botany*, **27**, 15–26.

Dennison WC, Orth RJ, Moore KA *et al.* (1993) Assessing water quality with submersed aquatic vegetation. *BioScience*, **43**, 86–94.

Dobson JE, Bright EA, Ferguson RL *et al.* (1995) *NOAA coastal change analysis program (C-CAP): guidance for regional implementation.* US Department of Commerce, National Oceanic and Atmospheric Administration, National Marine Fisheries Service.

Domestic Policy Council (2013) Technical Support Document:-Technical Update of the Social Cost of Carbon for Regulatory Impact Analysis-Under Executive Order 12866.

Douglass JG, France KE, Paul Richardson J, Duffy JE (2010) Seasonal and interannual changes in a Chesapeake Bay eelgrass community: insights into biotic and abiotic control of community structure. *Limnology and Oceanography*, **55**, 1499–1520.

Duarte CM, Cebrián J (1996) The fate of marine autotrophic production. *Limnology and Oceanography*, **41**, 1758–1766.

Duffy JE, Reynolds PL, Boström C *et al.* (2015) Biodiversity mediates top-down control in eelgrass ecosystems: a global comparative-experimental approach. *Ecology Letters*, **18**, 696–705.

Edgar GJ (1990) The use of the size structure of benthic macrofaunal communities to estimate faunal biomass and secondary production. *Journal of Experimental Marine Biology and Ecology*, **137**, 195–214.

Frederiksen M, Krause-Jensen D, Holmer M, Laursen JS (2004) Long-term changes in area distribution of eelgrass (*Zostera marina*) in Danish coastal waters. *Aquatic Botany*, **78**, 167–181.

Fromard F, Vega C, Proisy C (2004) Half a century of dynamic coastal change affecting mangrove shorelines of French Guiana. A case study based on remote sensing data analyses and field surveys. *Marine Geology*, **208**, 265–280.

Gallegos CL (2001) Calculating optical water quality targets to restore and protect submersed aquatic vegetation: overcoming problems in partitioning the diffuse attenuation coefficient for photosynthetically active radiation. *Estuaries*, **24**, 381–397.

Gardner TA, Cote IM, Gill JA, Grant A, Watkinson AR (2003) Long-term region-wide declines in Caribbean corals. *Science*, **301**, 958–960.

Giesen WBJT, Vankatwijk MM, Denhartog C (1990) Eelgrass condition and turbidity in the Dutch Wadden Sea. *Aquatic Botany*, **37**, 71–85.

Graham NAJ, Nash KL (2013) The importance of structural complexity in coral reef ecosystems. *Coral Reefs*, **32**, 315–326.

de Groot R, Brander L, van der Ploeg S *et al.* (2012) Global estimates of the value of ecosystems and their services in monetary units. *Ecosystem Services*, **1**, 50–61.

Gurbisz C, Kemp WM (2014) Unexpected resurgence of a large submersed plant bed in Chesapeake Bay: analysis of time series data. *Limnology and Oceanography*, **59**, 482–494.

Halpern BS, Walbridge S, Selkoe KA *et al.* (2008) A global map of human impact on marine ecosystems. *Science*, **319**, 948–952.

Jarvis JC, Moore KA (2010) The role of seedlings and seed bank viability in the recovery of Chesapeake Bay, USA, *Zostera marina* populations following a large-scale decline. *Hydrobiologia*, **649**, 55–68.

Jefferies RL, Jano AP, Abraham KF (2006) A biotic agent promotes large-scale catastrophic change in the coastal marshes of Hudson Bay. *Journal of Ecology*, **94**, 234–242.

Kemp MW, Batleson R, Bergstrom P *et al.* (2004) Habitat requirements for submerged aquatic vegetation in Chesapeake Bay: water quality, light regime, and physical-chemical factors. *Estuaries*, **27**, 363–377.

Kemp WM, Boynton WR, Adolf JE *et al.* (2005) Eutrophication of Chesapeake Bay: historical trends and ecological interactions. *Marine Ecology Progress Series*, **303**, 1–29.

Li X, Weller DE, Gallegos CL, Jordan TE, Kim H-C (2007) Effects of watershed and estuarine characteristics on the abundance of submerged aquatic vegetation in Chesapeake Bay subestuaries. *Estuaries and Coasts*, **30**, 840–854.

Lotze HK, Lenihan HS, Bourque BJ *et al.* (2006) Depletion, degradation, and recovery potential of estuaries and coastal seas. *Science*, **312**, 1806–1809.

Moore KA, Jarvis JC (2008) Environmental factors affecting recent summertime eelgrass diebacks in the lower Chesapeake Bay: implications for long-term persistence. *Journal of Coastal Research*, **Special Issue 55**, 135–147.

Moore KA, Shields EC, Parrish DB (2014) Impacts of varying estuarine temperature and light conditions on *Zostera marina* (eelgrass) and its interactions with *Ruppia maritima* (widgeongrass). *Estuaries and Coasts*, **37**, 20–30.

Najjar RG, Pyke CR, Beth M *et al.* (2010) Potential climate-change impacts on the Chesapeake Bay. *Estuarine, Coastal and Shelf Science*, **86**, 1–20.

NOAA Office of Science and Technology (2014) Annual Commercial Landing Statistics. Available at: https://www.st.nmfs.noaa.gov/pls/webpls/FT_HELP.SPECIES (accessed 22 August 2016).

Orth RJ, Moore KA (1983) Chesapeake Bay: an unprecedented decline in submerged aquatic vegetation. *Science*, **222**, 51–53.

Orth RJ, Moore KA (1984) Distribution and abundance of submerged aquatic vegetation in Chesapeake Bay: an historical perspective. *Estuaries*, **7**, 531–540.

Orth RJ, Moore KA (1986) Season and year-to-year variations in the growth of *Zostera marina* L. (eelgrass) in the lower Chesapeake Bay. *Aquatic Botany*, **24**, 335–341.

Orth RJ, Carruthers TJB, Dennison WC *et al.* (2006) A global crisis for seagrass ecosystems. *BioScience*, **56**, 987–996.

Orth RJ, Marion SR, Moore KA, Wilcox DJ (2010) Eelgrass (*Zostera marina* L.) in the Chesapeake Bay region of mid-Atlantic coast of the USA: challenges in conservation and restoration. *Estuaries and Coasts*, **33**, 139–150.

Orth RJ, Dennison WC, Lefcheck JS *et al.* (2017) Submersed aquatic vegetation in Chesapeake Bay: sentinel species in a changing world. In review.

Paine DP (1981) *Aerial photography and image interpretation for resource management.*

Patrick CJ, Weller DE (2015) Interannual variation in submerged aquatic vegetation and its relationship to water quality in subestuaries of Chesapeake Bay. *Marine Ecology Progress Series*, **537**, 121–135.

Patrick CJ, Weller DE, Li X, Ryder M (2014) Effects of shoreline alteration and other stressors on submerged aquatic vegetation in subestuaries of Chesapeake Bay and the mid-Atlantic coastal bays. *Estuaries and Coasts*, **37**, 1516–1531.

Patrick CJ, Weller DE, Ryder M (2016) The relationship between shoreline armoring and adjacent submerged aquatic vegetation in Chesapeake Bay and nearby Atlantic coastal bays. *Estuaries and Coasts*, **39**, 158–170.

R Development Core Team (2016) R: A Language and Environment for Statistical Computing.

Ralph GM, Seitz RD, Orth RJ, Knick KE, Lipcius RN (2013) Broad-scale association between seagrass cover and juvenile blue crab density in Chesapeake Bay. *Marine Ecology Progress Series*, **488**, 51–63.

Reusch TBH, Ehlers A, Hämmerli A, Worm B (2005) Ecosystem recovery after climatic extremes enhanced by genotypic diversity. *PNAS*, **102**, 2826–2831.

van Rij J, Wieling M, Baayen RH, van Rijn H (2016) itsadug: Interpreting Time Series and Autocorrelated Data Using GAMMs.

Ruhl HA, Rybicki NB (2010) Long-term reductions in anthropogenic nutrients link to improvements in Chesapeake Bay habitat. *PNAS*, **107**, 16566–16570.

Rybicki NB, Landwehr JM (2007) Long-term changes in abundance and diversity of macrophyte and waterfowl populations in an estuary with exotic macrophytes and improving water quality. *Limnology and Oceanography*, **52**, 1195–1207.

Short FT, Wyllie-Echeverria S (1996) Natural and human-induced disturbance of seagrasses. *Environmental Conservation*, **23**, 17.

Sobocinski KL, Latour RJ (2015) Trophic transfer in seagrass systems : estimating seasonal production of an abundant seagrass fish, Bairdiella chrysoura, in lower Chesapeake Bay. *Marine Ecology Progress Series*, **523**, 157–174.

Waycott M, Duarte CM, Carruthers TJB *et al.* (2009) Accelerating loss of seagrasses across the globe threatens coastal ecosystems. *PNAS*, **106**, 12377–12381.

Wernberg T, Bennett S, Babcock RC *et al.* (2016) Climate-driven regime shift of a temperate marine ecosystem. *Science*, **353**, 169–172.

Wood SN (2011) Fast stable restricted maximum likelihood and marginal likelihood estimation of semiparametric generalized linear models. *Journal of the Royal Statistical Society B*, **73**, 3–36.

Zimmerman RC (2006) Light and photosynthesis in seagrass meadows. In: *Seagrasses: Biology, Ecology, and Conservation* (eds Larkum AWD, Orth RJ, Duarte CM), pp. 303–321. Springer, Dordrecht, The Netherlands.

Zimmerman RC, Smith RD, Alberte RS (1989) Thermal acclimation and whole-plant carbon balance in *Zostera marina* L. (eelgrass). *Journal of Experimental Marine Biology and Ecology*, **130**, 93–109.

Supporting Information

Additional Supporting Information may be found in the online version of this article:

Figure S1 The locations of eelgrass beds (red) and water quality monitoring stations (black dots) used in the analysis.

Figure S2 Significant predictors of eelgrass cover for multiple depth strata.

Appendix S1 Lefcheck_2017_GCB_Analysis.R – an R script used to exactly reproduce the analysis contained in the main text and supplements.

Appendix S2 EvaluateSmooths. R – Supplementary R function called by *Lefcheck_2017_GCB_Analysis.R*.

Appendix S3 Lefcheck_2017_GCB_Eelgrass_Area.csv – A data file containing the total seagrass area (in hectares) for each 'subregion' in each year.